npj | urban sustainability

Article

Published in partnership with RMIT University

https://doi.org/10.1038/s42949-026-00353-w

Modeling urban planning contributions to flood resilience under shared socioeconomic pathways

Check for updates

Wenhan Feng[1] ✉, Yimeng Liu[2], Anqi Zhu[1], Junqi Mao[3], Tianyi Sun[4], Qingsong Xu[5], Yuhan Yang[6], Hao Su[1], Wenhao Wu[7], Qiqi Yang[8], Alistair Ford[2], Matthias Garschagen[1] & Liang Emlyn Yang[1] ✉

Flooding from short-duration extreme rainfall poses growing risks to rapidly urbanizing regions under climate change. This study integrates 2035 urban planning into simulations of extreme rainfall-induced flooding in the Pearl River Delta Metropolitan region. Results show that while urban planning has limited impact on reducing overall hazard, it plays a critical role in redistributing it spatially. Flood hazard and exposure in 2035 were assessed under four Shared Socioeconomic Pathways (SSPs). Hazard decreases by about 10% in SSP1, remains stable in SSP2, and rises in SSP3 and SSP5, with SSP5 showing a 12% increase. Population exposure grows across all scenarios, with increases of 21% in SSP1, 25% in SSP2, 13% in SSP3, and 56% in SSP5. Asset exposure shows even larger increases, from 29% in SSP3 to more than 100% in SSP5. These results highlight that while urban planning can alleviate hazard locally, long-term resilience is dominated by socioeconomic development trajectories.

One of the key tasks of current climate action is to evaluate existing adaptation practices and integrate them into policy-making to effectively guide future climate strategies[1–4]. In response, the scientific community has produced a number of comprehensive reviews based on large-scale analyses of the academic literature[3,5–7]. These efforts provide a holistic perspective on how adaptation is understood and discussed in scientific research.

However, such studies often lack direct evidence from government planning and reports. The disconnect between scholars and policymakers has been long evident and is particularly pronounced in the field of urban planning[8]. Traditional urban planning is rooted in architecture and design, involving a large number of practitioners, engineers, and designers who tend to operate outside of academic discourse. This has led to a gap between urban planning practice and scholarly narratives in scientific literature. For example, despite increasing academic advocacy for nature-based solutions, decision-makers in practice often prioritize pragmatic factors, such as regulatory obligations, budget constraints, and implementation capacity, over insights from scientific research[9–11]. This mismatch highlights how academic recommendations may overlook the institutional and operational realities faced by planning agencies[12,13].

Two main research approaches have partially addressed this gap: (1) conceptual analyses of policy documents, which focus on text-based policy assessment[14–16], and (2) quantitative evaluations of specific adaptation measures(e.g., green infrastructure) that assess feasibility and effectiveness at localized scales[17–20]. The former offers conceptual insights on broader scales but often lacks detailed consideration of localized practices, particularly in terms of the spatial configuration of adaptation measures. The latter helps to fill this gap but typically relies on hypothetical or expert-defined adaptation scenarios that may not fully reflect real-world governance contexts. Consequently, a systematic assessment of how actual governance systems and planning practices influence future climate risks remains absent.

The rapid increase in flood risk driven by climate change and urbanization is widely acknowledged. At the same time, systems of social governance continue to evolve rather than remain static, reflecting the long-term resilience of human societies[21–23]. Despite differing political cultures and traditions across countries, there is a common understanding that it is a governmental responsibility to safeguard public welfare[7,24,25]. Governments at different levels around the globe are taking active steps to address escalating flood risks[26]. The urban planning system (including master plans,

[1]Department of Geography, Ludwig Maximilian University of Munich (LMU), Munich, Germany. [2]DARe hub, School of Engineering, Newcastle University, Newcastle, UK. [3]School of Environment and Energy, Peking University Shenzhen Graduate School, Shenzhen, China. [4]School of Ecology & Environment, Renmin University of China, Beijing, China. [5]TUM School of Engineering and Design, Technical University of Munich, Munich, Germany. [6]School of Emergency Management, Nanjing University of Information Science & Technology, Nanjing, China. [7]Department of Environmental Science and Engineering, Fudan University, Shanghai, China. [8]City Design Institute, Guangdong Urban & Rural Planning and Design Institute, Guangzhou, China.
✉e-mail: wenhan.feng@geographie.uni-muenchen.de; emlyn.yang@lmu.de

land use plans, and various types of infrastructure-focused sectoral plans) reflects governmental visions for the future and embeds targeted risk management strategies[27].

In most current climate change impact and adaptation modeling, future risks are simulated without incorporating existing planning frameworks, and studies often conclude with broad recommendations to integrate climate adaptation into urban planning[28–30]. This overlooks the fact that many planning systems already include risk reduction and adaptation measures with clear policy implications[31–33]. For example, regional flood control masterplans and ecological restoration projects are widely implemented in Chinese cities but remain largely absent in quantitative climate-risk models.

In the absence of consideration for government planning strategies, regions such as the Netherlands, the United Kingdom, the southeastern United States, and central China are often projected to experience large increases in risk[34], whereas actual loss data trends in those regions often paint a more nuanced picture[35]. While these areas are expected to maintain high population densities, which is a major driver of risk increase, local governments are continuously advancing flood adaptation plans and investments, which themselves serve as important sources of safety and may partially explain continued population concentration[27]. Understanding whether such safety provisions are sufficient, how they can be improved, or whether gaps in implementation exist is a far more practical question. Therefore, rather than simply providing vague warnings, it is necessary to assess these safety mechanisms quantitatively.

Furthermore, Shared Socioeconomic Pathway (SSP), as a core framework in global change research, has increasingly been applied to local and regional studies in recent years[36,37]. These applications are often achieved through downscaling methods that link global SSP scenarios with local socioeconomic characteristics, urban development trends, and governance capacities to better reflect regional heterogeneity and dynamic processes[36,38,39]. However, most SSP-based downscaling studies tend to use current conditions or land use modeling results as the simulation basis and often lack explicit consideration of actual governmental planning[40–42]. This is often due to a combination of limited access to urban planning data, difficulty in translating policy intentions into spatial parameters, and a lack of interdisciplinary collaboration between urban planners and modeling communities. As a result, the underlying spatial impacts of planning measures are often underestimated. There is a growing need for interdisciplinary efforts to integrate urban planning into future scenario modeling and to systematically assess its potential contributions to climate risk reduction.

The Pearl River Delta Metropolitan (PRDM) region offers a particularly relevant case for this inquiry. As one of the most rapidly urbanizing areas in the world, the PRDM faces intense land development pressures and increasing exposure to short-duration extreme rainfall events. At the same time, it has a relatively comprehensive urban planning system, including proactive ecological, hydrological, and infrastructural measures that aim to reduce flood risks. These characteristics make the PRDM an insightful example for assessing how planning interventions interact with broader socioeconomic trajectories in shaping future flood resilience.

Bear these concerns in mind, we investigate whether, and to what extent, urban planning can help mitigate future flood risks under the assumption of effective implementation. Focusing on the PRDM region in China, we collected and synthesized a comprehensive set of existing local planning measures, including ecological restoration projects, hydrological modifications, and flood storage and drainage infrastructure. We simulated flood hazard and associated population and asset exposure under four SSP scenarios in the year 2035, comparing these results with current conditions. Through this spatial assessment, we evaluated the effectiveness of urban planning in the PRDM and provided policy-relevant insights.

This paper offers four main contributions:

1. It incorporates real-world planning measures into the SSP framework, quantifying the coupled effects of local governance, policy intervention, and socioeconomic development on future flood risk.
2. It develops a multi-scale modeling framework that bridges the gap between policy texts and on-the-ground adaptation practices, from grid-level to metropolitan scale.
3. It integrates diverse open-source datasets and spatial analytical methods to propose a systematic approach for including planning interventions in SSP-based downscaled flood exposure assessments.
4. It provides a spatially explicit evaluation of how actual urban planning affects flood hazard and exposure across scenarios, enriching the representation of projected adaptation measures and their effects.

Results

Governance structures for flood-related urban planning in China

In the PRDM, flood-related urban planning involves multiple local government departments, requiring coordination and interdepartmental collaboration (Fig. 1). At the county or district level, agencies responsible for areas such as urban development, water management, spatial planning, ecological protection, economic strategy, and disaster response jointly form a multi-sectoral governance network. The planning system operates at three levels: (1) overarching comprehensive plans that set general development and adaptation goals; (2) sectoral plans targeting specific areas like flood control, sponge city construction, and emergency management; and (3) technical guidelines that provide design standards to support implementation.

These three levels of planning are coordinated both vertically and horizontally. Comprehensive plans typically provide guidance and constraints for sectoral plans, while the latter must be mutually consistent in their spatial content and policy objectives. Within this structure, the 14th Five-Year Plan plays a particularly influential role. It is not only a central document guiding regional development but is also frequently used as the basis or justification for other plans (as shown by the blue line in Fig. 1). This structure helps connect broad development strategies with specific adaptation actions.

However, in practice, the implementation of such multi-level plans often faces challenges due to overlapping departmental responsibilities and fragmented governance structures. Multiple agencies, such as those in water management, land use, and ecological protection, often operate under separate mandates and funding arrangements. This can hinder effective coordination. Misalignments may arise when one department's flood control objectives conflict with another department's environmental or spatial development goals. Despite these coordination challenges, existing planning documents still provide a valuable basis for understanding the spatial strategies adopted for flood governance.

We compiled flood governance measures with explicit spatial references from the urban planning documents outlined in Fig. 1, covering cities across the PRDM, as summarized in Fig. 2. These measures span a range of domains, including hydraulic engineering, urban drainage systems, green infrastructure, and ecological protection. They reflect how different sectoral plans are translated into spatial strategies and interventions.

Specifically, reservoirs, pumping stations, drainage channels, and newly constructed rivers are mainly concentrated in low-lying or flood-prone areas such as the western bank of the Pearl River and core urban districts. This distribution indicates that flood prevention and drainage plans prioritize regional water discharge safety in these zones. Drainage system upgrades are primarily located in older urban centers and are closely tied to underground space utilization and urban renewal plans, aiming to improve runoff capacity in densely built-up areas. In terms of green infrastructure, infiltration-enhanced zones for sponge city construction are concentrated in pilot areas of Guangzhou, Shenzhen, and Foshan City. These interventions are designed to reduce peak runoff through increased surface permeability and temporary water storage. Wetland parks, urban greenways, and ecological corridors are widely distributed across urban–rural interfaces and ecological control zones. They serve as core components of ecological restoration and urban renewal strategies while providing natural buffer zones against extreme precipitation events.

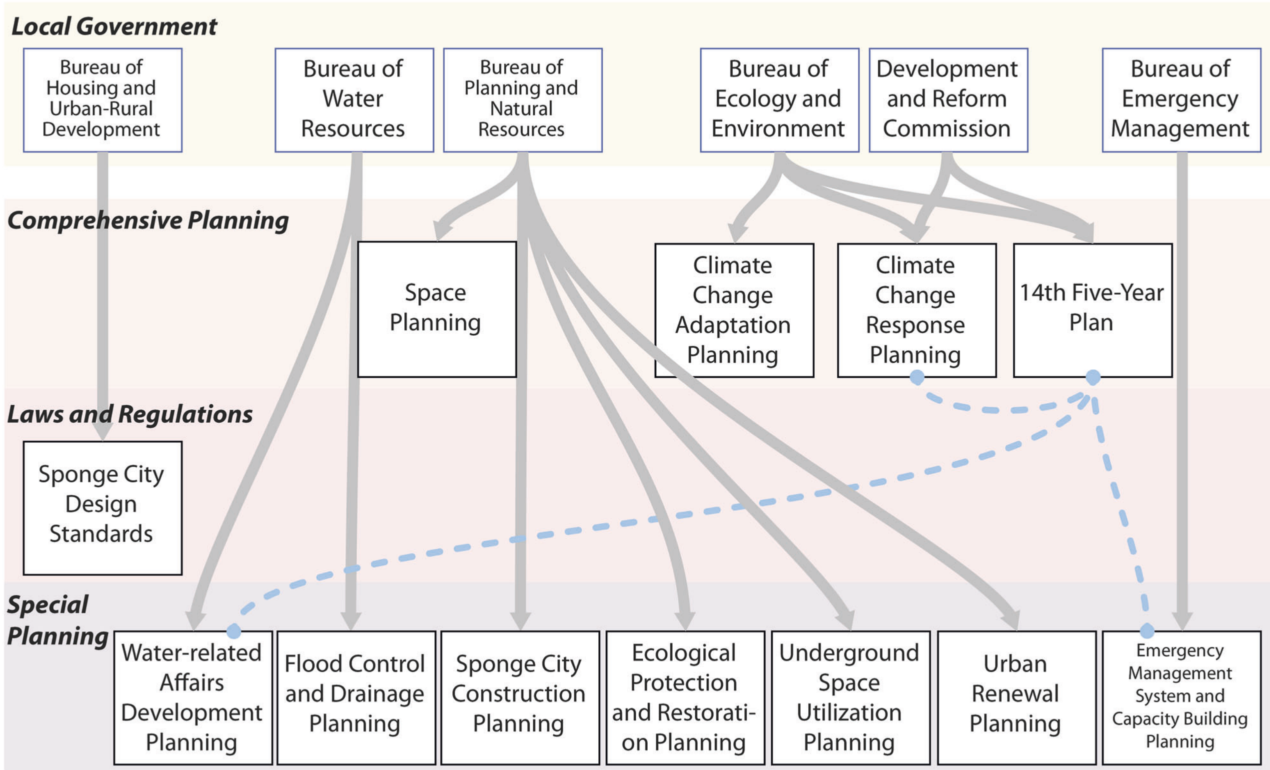

Fig. 1 | Urban planning system for flood governance in the PRDM. This figure shows the multi-sectoral planning system for flood governance in the PRDM.

These measures vary in type and institutional origin, illustrating their functional complementarity and serving as spatial expressions of the governance structure. Together, they represent the main planning foundation for flood risk management in the PRDM and provide essential inputs for the scenario simulations and risk assessments in this study.

The role of urban planning

We first analyzed flood hazard for 2035 under the SSP2 scenario, comparing conditions with and without urban planning measures. We used a simulation based on 2022 land-cover and SSP2 climate, population, and socioeconomic inputs as the baseline scenario, against which the two 2035 scenarios were compared. The two 2035 scenarios share the same SSP2 projections and differ only in land-cover inputs. We evaluated flood hazard using maximum inundation depth, and Fig. 3 presents hazard ratios relative to the baseline. A hazard ratio of 1 indicates no change, and values above 1 indicate increases.

Figure 3a shows the hazard ratio distribution at the grid-cell level. In the absence of planning, the median hazard ratio is 1.008, indicating a slight upward trend. With planning, the median remains unchanged, but the share of cells with hazard ratios > 1 is slightly smaller, suggesting that while the overall trend remains unchanged, the increase in risk has been mitigated in some areas. This is further reflected in the cumulative statistics in Fig. 3b, which compares the proportions of areas where hazard ratio is ≤ 1 (reduced or unchanged) and > 1. Although the reduction is limited, it shows that urban planning has produced a localized buffering effect.

Subtracting the hazard values of the no-planning scenario from those of the planning scenario, each grid cell was categorized into one of three groups: "greater hazard under planning," "no difference," and "lower hazard under planning," as illustrated in Fig. 4.

Most areas in the PRDM (shown in yellow) exhibit no significant difference in simulated flood hazard between the two scenarios. These are primarily located in non-urbanized or higher-elevation regions. Areas that are better protected under the planning scenario (shown in blue) are concentrated in core or sub-core urban districts. These locations are typically covered by a variety of planning interventions, including drainage infrastructure upgrades, permeable pavement, and greenway construction.

In addition, certain areas (shown in red) experience greater simulated inundation under the planning scenario, primarily located in urban expansion zones. A comparison between the high hazard ratio areas in Fig. 4 and the spatial layout of greenways and ecological restoration zones in Fig. 2 reveals that some of the newly inundated locations coincide with areas of high infiltration capacity, such as the ecological buffer zone in northern Guangzhou, the greenway corridor in central Dongguan, and the ecological restoration zone in northwestern Shenzhen. These zones are intended to capture and temporarily store excess surface runoff during extreme rainfall events, which helps relieve flood pressure on adjacent built-up areas. Therefore, although hazard levels may rise in some locations, more densely developed regions benefit from a buffering effect provided by these spatial interventions.

To further investigate the relationship between planning measures and changes in flood hazard, we analyzed the correlation between the proportion of areas exhibiting smaller or larger hazard under the planning scenario (relative to the no-planning scenario) and the spatial coverage of planning interventions within each county or district. In Fig. 5, blue points represent areas with smaller hazard under the planning scenario, while red points represent areas with larger hazard.

Regression analysis reveals statistically significant positive correlations in both cases. For zones with larger hazard, the slope is 0.85, indicating that a 10% increase in planning coverage is associated with an 8.5% increase in the proportion of affected zones. $R^2 = 0.51$ indicates that planning coverage explains about half of the variance, and the p-value (<0.001; $p = 3.01 \times 10^{-8}$) confirms the significance of this relationship. For zones with smaller hazard, the slope is 0.67, with $R^2 = 0.42$ and $p < 0.001$ ($p = 1.25 \times 10^{-5}$), also indicating a significant association.

These findings suggest that as planning coverage increases, the proportions of both larger- and smaller-hazard zones tend to rise, reflecting a hydrological redistribution effect. It can be inferred that planning measures

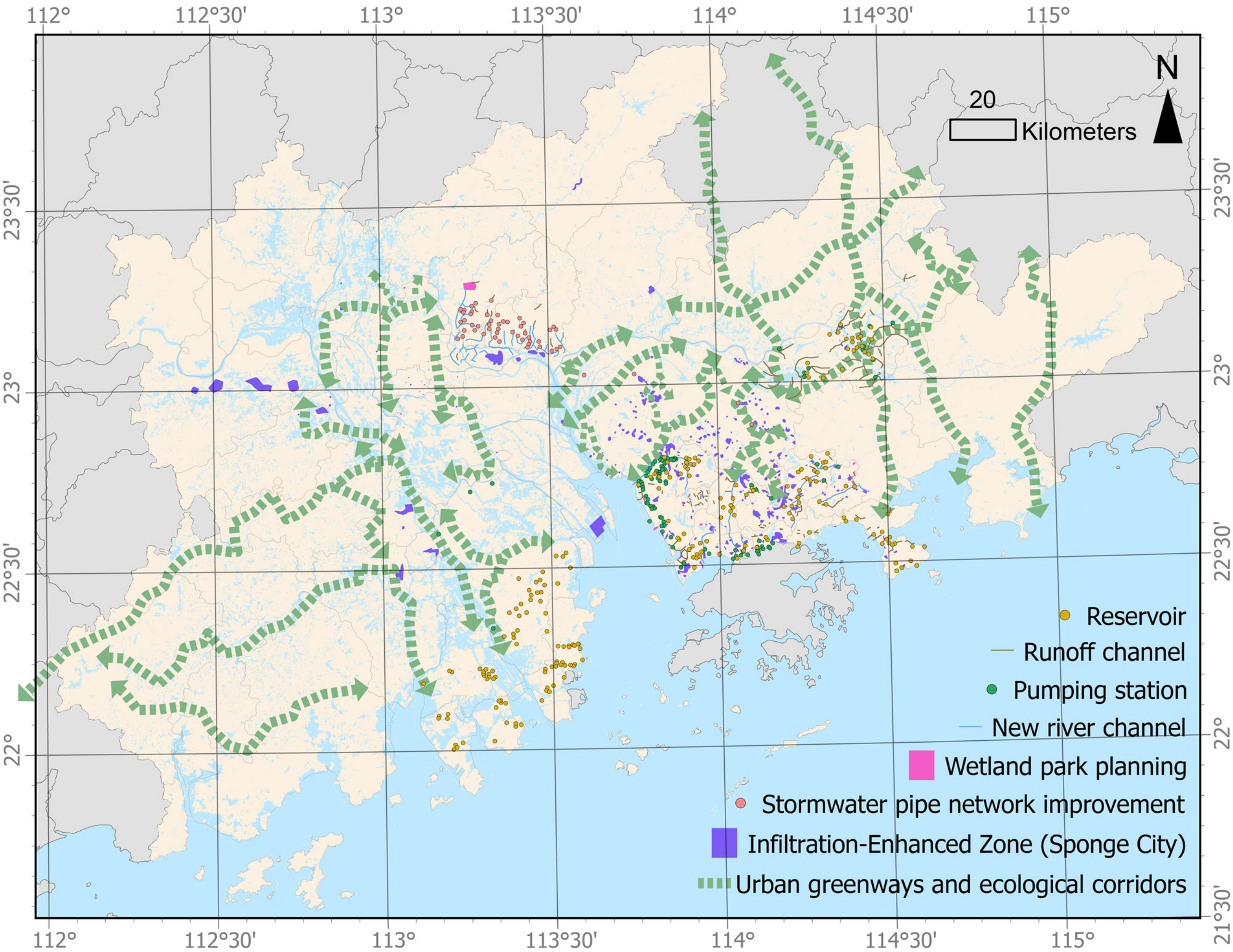

Fig. 2 | Flood-related urban planning measures in the PRDM by 2035. This figure shows the spatially referenced flood-related urban planning measures across PRDM cities projected for 2035.

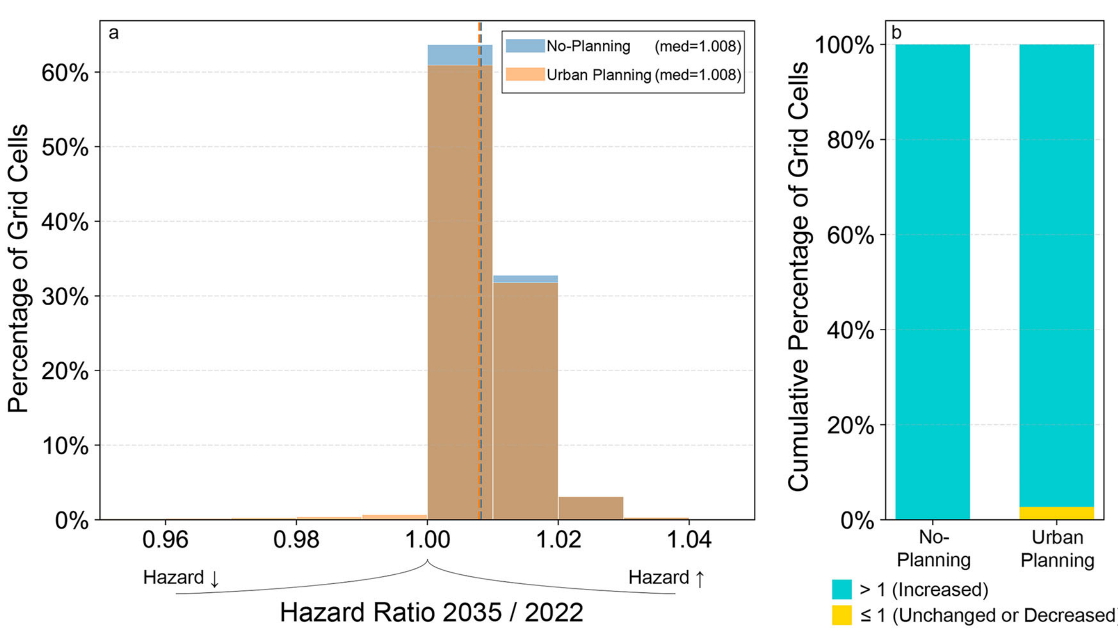

Fig. 3 | Hazard differences between planning and no-planning scenarios. This figure shows the comparison of hazard ratios under planning and no-planning scenarios relative to the 2022 baseline: **a** histogram of hazard ratio distribution at the grid-cell level, and **b** cumulative statistics comparing the proportions of areas with hazard ratio ≤1 and >1.

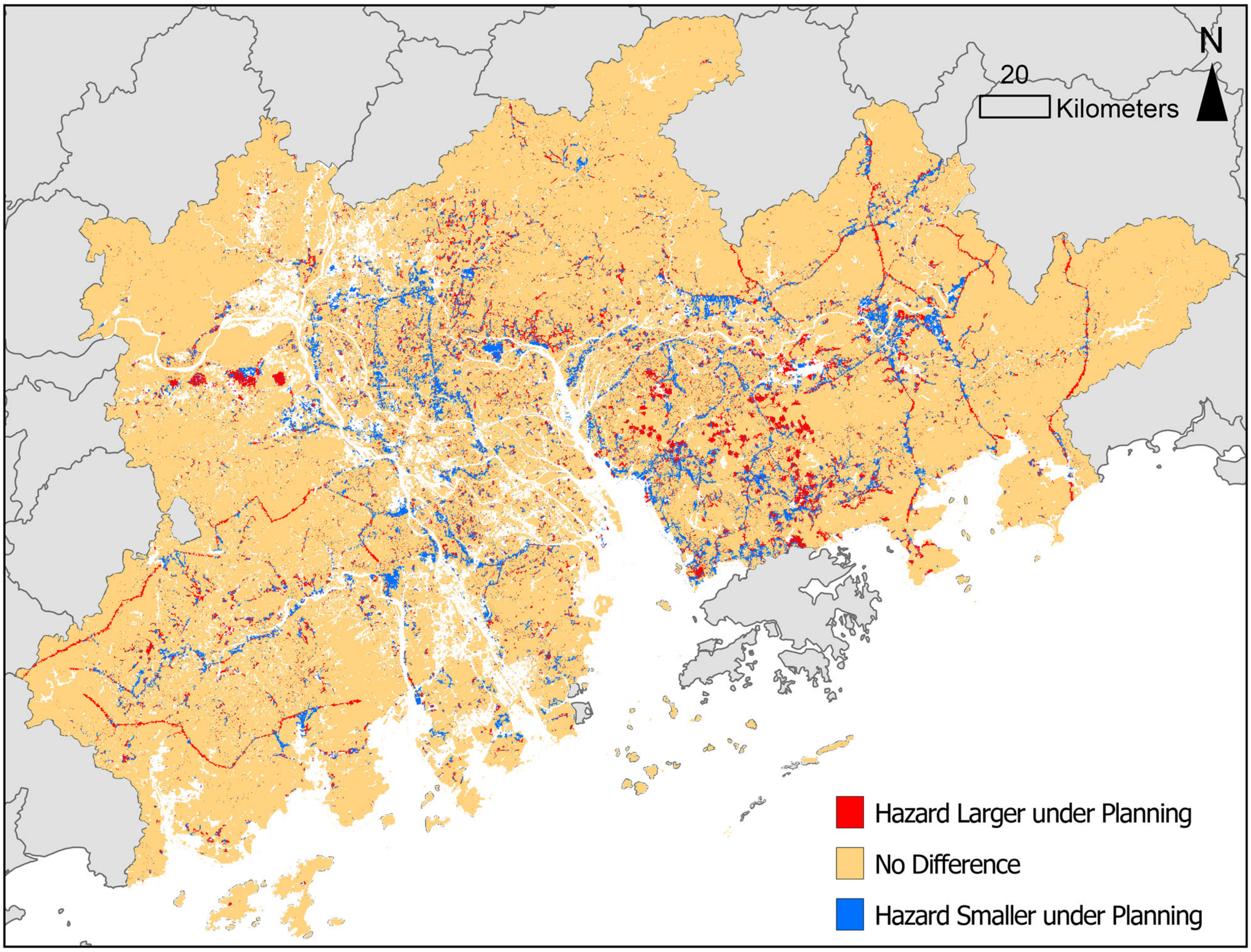

Fig. 4 | Spatial distribution of hazard differences between planning and no-planning scenarios. This figure shows the spatial distribution of grid cells classified as greater hazard, no difference, or lower hazard under planning compared to the no-planning scenario.

Fig. 5 | Relationship between planning coverage and flood hazard changes. This figure shows the correlations between planning coverage and the proportions of areas with smaller hazard (blue points) and larger hazard (red points) under the planning scenario compared to the no-planning scenario.

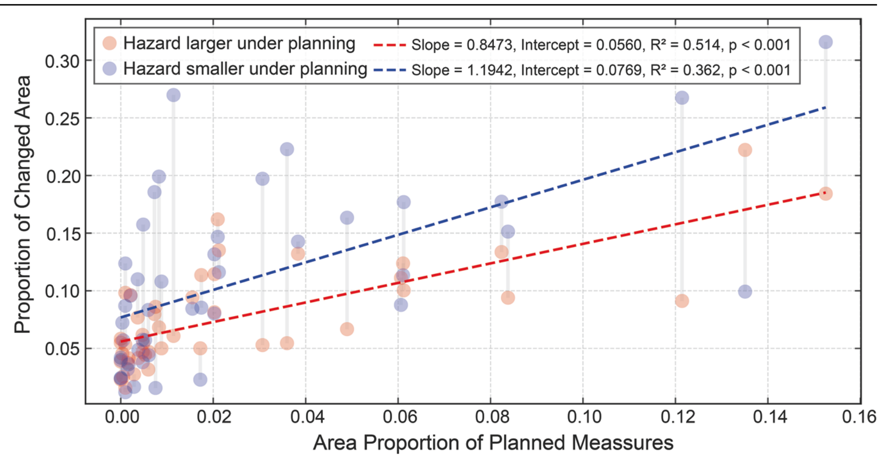

may reduce flood hazard in some areas while unintentionally increasing it in others, resulting in spatial trade-offs that need to be considered in adaptive planning. Whether such redistribution is beneficial depends on whether excess water is directed to absorptive zones or to vulnerable areas. Nonetheless, the fitted regression for zones with smaller hazard shows a higher slope and intercept than that for zones with larger hazard, indicating that the proportion of zones with smaller hazard consistently exceeds that of zones with larger hazard. This suggests that planning interventions produce a net mitigation effect. Moreover, this effect becomes more pronounced as planning coverage increases.

Overall, urban planning shows mitigation potential, though with uneven spatial effects due to hydrological reconfiguration. This adjustment does not equate directly to risk reduction, but rather involves internal structural reorganization and the redistribution of localized trade-offs. The magnitude of this effect increases with the extent of implemented planning measures.

SSP scenario simulations of future hazard and exposure changes with urban planning

We assessed future flood hazard and exposure under four SSP scenarios with urban planning included. The 2022 SSP2 scenario was used as the baseline. Hazard, population exposure, and asset exposure are expressed as cell-level ratios of 2035 values relative to the baseline.

Figure 6a presents histograms of hazard ratio values at the grid-cell level for each scenario. The results show clear differences across scenarios. Under SSP1, which reflects a pathway of green transition and reduced resource-intensive development, flood hazard decreases by approximately 10.5% (median: 0.895). SSP2 remains largely stable, with only a slight increase of about 0.8% (median: 1.008). In contrast, SSP3 and SSP5 show rising trends, with increases of 2.7% (median: 1.027) and 12.1% (median: 1.121), respectively, suggesting that scenarios characterized by high emissions, rapid urban expansion, and limited governance capacity are associated with greater flood hazard intensification.

The dispersion of hazard ratios also differs across scenarios. The distribution of grid cell values in SSP3 is the most concentrated, followed by SSP2, whereas SSP1 and SSP5 exhibit more dispersed patterns. Figure 6b shows that most SSP1 grid cells have hazard ratios ≤ 1, suggesting that flood risk has decreased across many areas relative to 2022. In contrast, SSP2, SSP3, and SSP5 show a clear dominance of areas with increasing hazard levels.

Figure 6c–f show the spatial patterns of hazard changes. In SSP1, many areas exhibit significant reductions in flood hazard, particularly in the northern mountainous zones and the outskirts of urban areas. In SSP2, most urban areas show hazard ratio values between 1 and 1.15, indicating a slight overall increase. In SSP3 and SSP5, the spatial spread of flood hazard is noticeably more severe. This is particularly evident in SSP5, where large portions of the region are covered by orange and red zones, reflecting widespread increases in hazard. This pattern illustrates that under the combined effects of intensified climate change and accelerated urban development, the effectiveness of current planning measures in mitigating flood hazard is limited.

Figure 7 illustrates the changes in flood population exposure in 2035 under the four SSP scenarios, relative to the baseline. Population exposure is expressed as the ratio of 2035 to 2022 values. As shown in Fig. 7a, the median population exposure ratio exhibits a systematic upward trend across all SSP scenarios, with notable differences between them: SSP1 shows an increase of 21.3% (median: 1.213); SSP2 rises by 24.8% (median: 1.248); SSP3 increases by 12.9% (median: 1.129); and SSP5 shows the highest growth at 55.7% (median: 1.557). It is worth noting that although flood hazard ratio in SSP3 (as seen in Fig. 6) is slightly higher than in SSP2, its median population exposure ratio is lower, suggesting that population clustering in high-hazard areas is relatively less pronounced in SSP3 compared to SSP2. This reflects the influence of socioeconomic pathways on population distribution.

Figure 7b shows the proportion of grid cells with increased (exposure ratio > 1) or reduced (≤1) exposure across scenarios. In SSP1, over 30% of cells show reduced exposure, whereas in SSP5 more than 90% show increases. Additionally, although SSP1 contains the largest number of cells with reduced population exposure, the values are widely dispersed, resulting in a higher median than the more concentrated SSP3.

The spatial maps in Fig. 7c–f further reveal the geographic distribution of exposure changes. In SSP1 (Fig. 7c), increased population exposure is primarily located at the urban fringes in the central and eastern parts of the region, with limited change in core urban areas. In SSP2 (Fig. 7d) and SSP3 (Fig. 7e), the extent of population exposure expands to cover more urban areas, but the overall intensity in peripheral zones is weaker compared to SSP1. In SSP5 (Fig. 7f), high population exposure areas are widely distributed.

Figure 8 illustrates the changes in flood asset exposure in 2035 under the four SSP scenarios, with urban planning considered. As shown in Fig. 8a, the median asset exposure ratio across all scenarios is clearly greater than 1, indicating a systemic increase in flood asset exposure under future socioeconomic expansion. The increases are 45.6% (median: 1.456) for SSP1, 40.2% (median: 1.402) for SSP2, and 29.2% (median: 1.292) for SSP3, while SSP5 shows the highest increase at 104.6% (median: 2.046), significantly exceeding the other scenarios. Although SSP1 involves reduced hazard levels due to mitigation and sustainability goals (as seen in Fig. 6), its rapid projected GDP growth still leads to a substantial increase in asset exposure. Conversely, SSP3 has the lowest median asset exposure ratio, indicating that despite elevated flood hazard, slower economic growth under this scenario limits the overall rise in asset exposure. In all scenarios, areas with reduced asset exposure are very limited (Fig. 8b).

Figure 8c–f present the spatial distribution of asset exposure ratios for each scenario. In SSP1 (Fig. 8c), areas with high asset exposure growth (>50%) are widely distributed across urban regions, while some mountainous areas remain at original asset exposure levels. In SSP2 and SSP3 (Fig. 8d, e), high asset exposure growth is observed only in urban peripheries and ecological restoration zones, highlighting potential conflicts between ecological conservation and economic development. Under SSP5 (Fig. 8f), asset exposure ratios exceed 2 across almost the entire PRDM, forming a clear pattern of widespread exposure accumulation.

The regulatory capacity of urban planning on exposure is relatively limited. Even with the inclusion of green infrastructure and risk reduction measures, the total increase in exposure is difficult to constrain. This is evident even under SSP1, where hazard ratio levels are generally lower, but the spatial extent of hazard-affected areas won't be substantially reduced. As long as people and assets continue to occupy these areas, exposure remains considerable. The challenge becomes even more pronounced under SSP5, where rapid economic expansion is coupled with a substantial increase in flood hazard, highlighting the need for urban planning to be more closely aligned with broader development trajectories in order to support effective disaster risk management. Therefore, the simulation results suggest that urban planning has some potential to counteract the increasing trend of flood hazard. However, its effectiveness strongly depends on the broader socioeconomic context.

Discussion

The preceding analysis shows that under future scenarios, sustainability-oriented pathways such as SSP1 are associated with relatively lower levels of risk and exposure, highlighting their potential for long-term risk reduction. However, the prospect of achieving such pathways is becoming increasingly uncertain. Beyond our model findings, recent assessments indicate a high likelihood that global temperatures will temporarily exceed the 1.5 °C threshold within the next few years[43], raising doubts about the feasibility of low-emission scenarios such as SSP1[44]. Nevertheless, across different development trajectories, urban planning still demonstrates potential to mitigate flood risks, thereby further substantiating the critical role of government policies in enhancing urban resilience[45,46].

In our simulations, urban planning has helped mitigate the rising trend of flood hazards in some high-density built-up areas by reshaping local hydrodynamics. Although some of these high-infiltration zones display locally increased water accumulation, this is primarily a result of flow redistribution. Floodwaters are redirected to temporarily absorptive areas, thereby indirectly relieving the pressure on surrounding built-up zones. These simulation-based patterns are consistent with the growing consensus in the literature that ecological spaces embedded in the planning, such as greenway systems, ecological restoration zones, and wetland parks, serve significant hydrological buffering functions[47–49].

As highlighted in the broader literature, this mechanism reduces risk in densely built zones by diverting floodwater to planned absorptive spaces, aligning with the concept of floodable areas proposed by Liao[50] as a surrogate measure of urban flood resilience. These areas are intentionally designed to tolerate and store excess water, enabling cities to manage floods through controlled inundation and ecological adaptation. This spatial strategy resonates with broader nature-based approaches to flood risk reduction. In this regard, Chen et al.[51] further emphasize that reducing the interconnection of flood risk patches through nature-based solutions, as illustrated by China's sponge city initiatives, is critical for

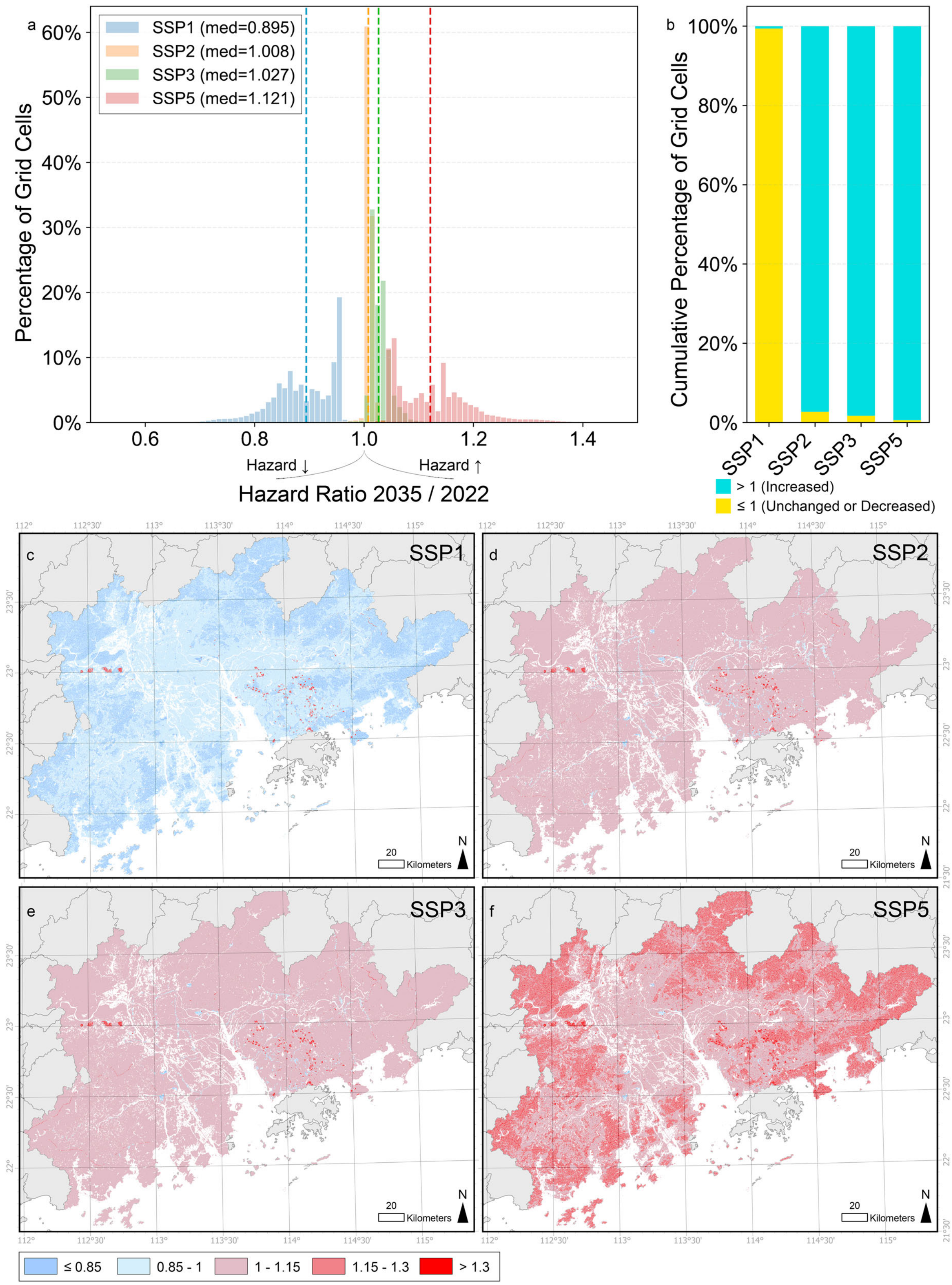

Fig. 6 | Hazard changes under four SSP scenarios in 2035 with urban planning considered. This figure shows flood hazard changes relative to the baseline: **a** histograms of hazard ratio values for each SSP scenario, **b** cumulative distributions of hazard ratios, and (**c**–**f**) spatial distributions of hazard ratios for SSP1, SSP2, SSP3, and SSP5, respectively.

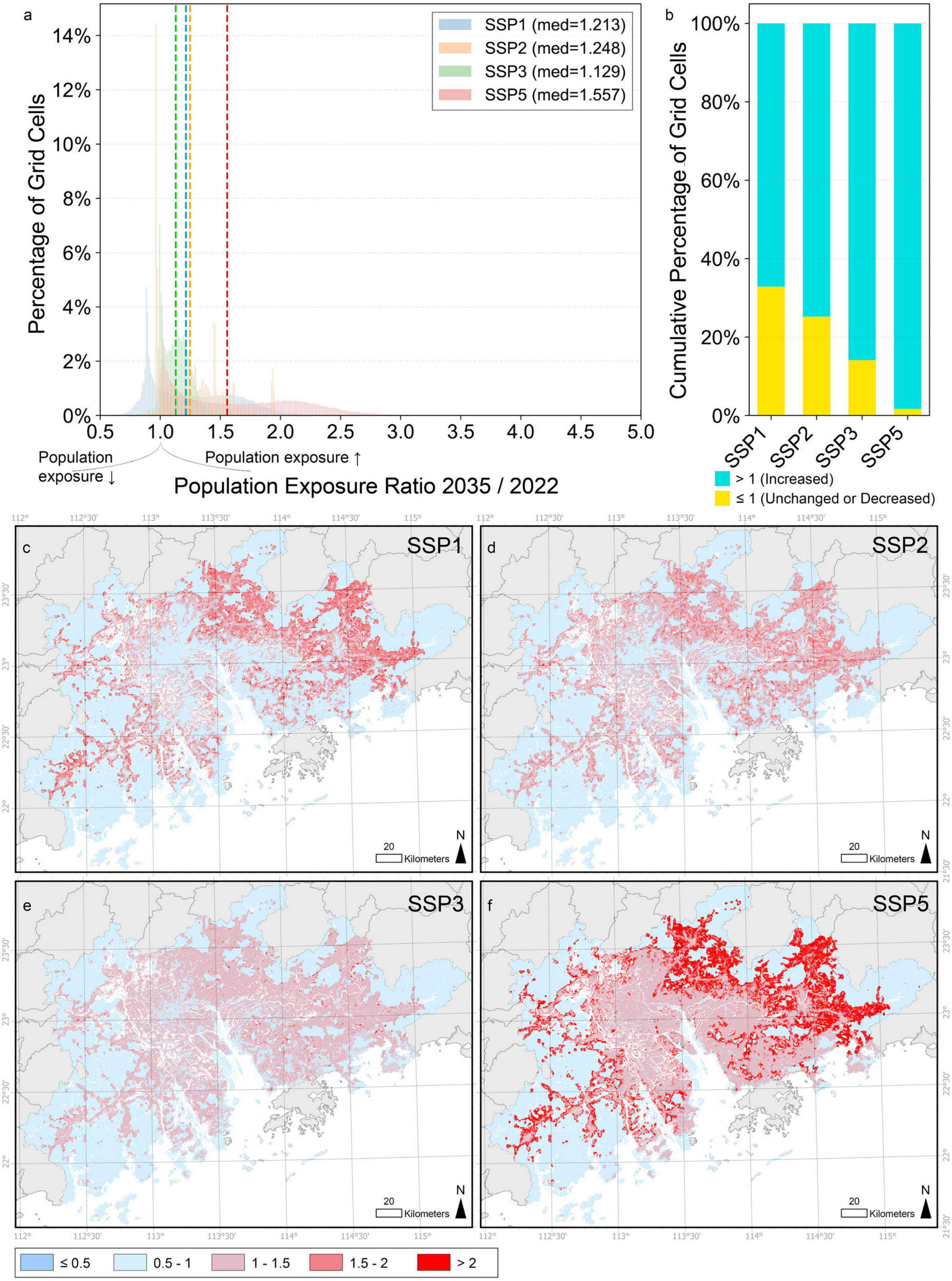

Fig. 7 | Changes in flood population exposure in 2035 under four SSP scenarios with urban planning considered. This figure shows changes in population exposure relative to the baseline: **a** histograms of exposure ratio values, **b** proportions of grid cells with increased or reduced exposure, and (**c**–**f**) spatial distributions of population exposure ratios for SSP1, SSP2, SSP3, and SSP5, respectively.

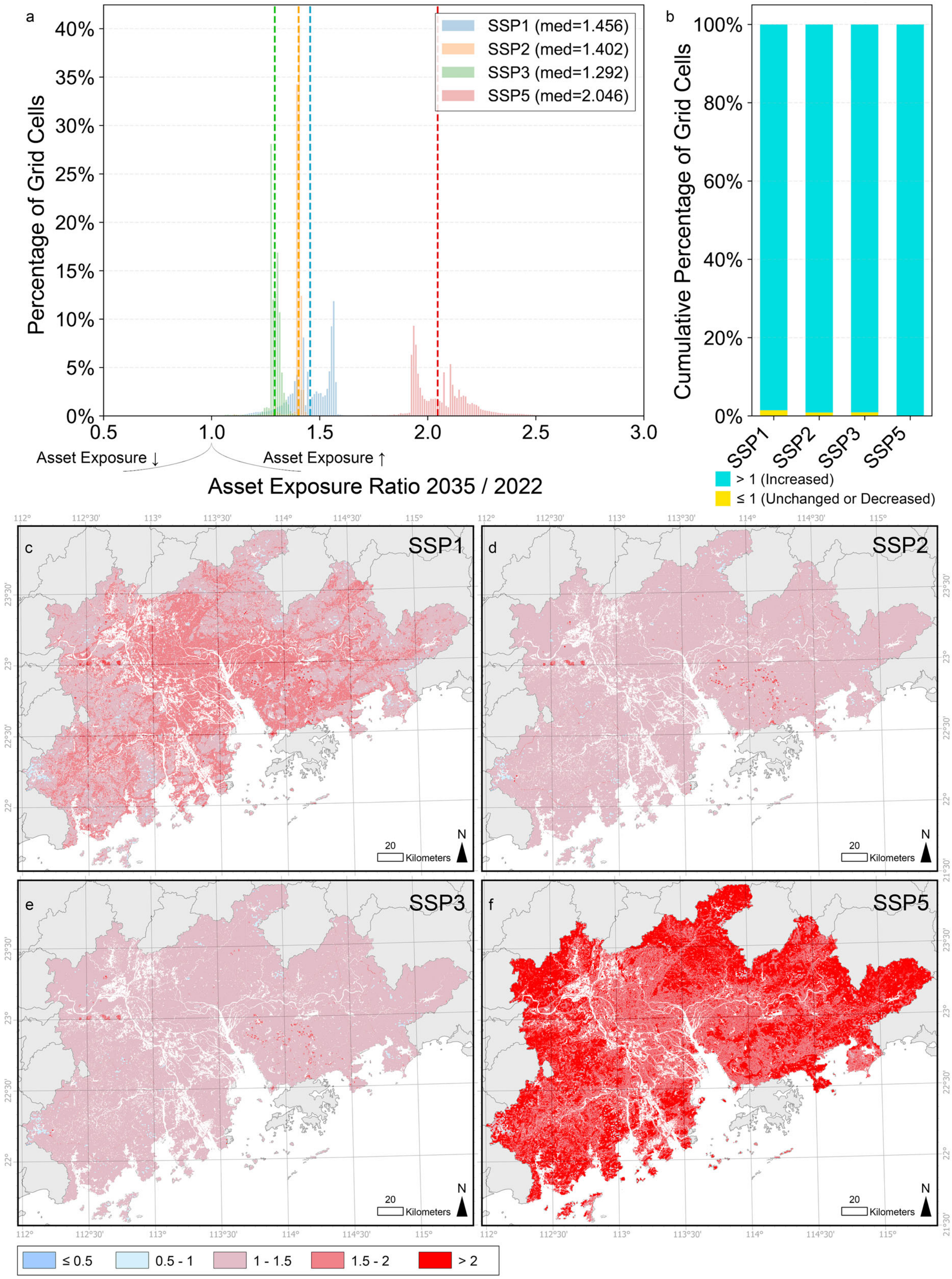

Fig. 8 | Changes in flood asset exposure in 2035 under the four SSP scenarios with urban planning considered. This figure shows changes in asset exposure relative to the baseline: **a** histograms of asset exposure ratios, **b** proportions of grid cells with increased or reduced exposure, and (**c**–**f**) spatial distributions of asset exposure ratios for SSP1, SSP2, SSP3, and SSP5, respectively.

compartmentalizing flood impacts. Evidence from Asian mega-deltas also highlights the cost-effectiveness of nature-based solutions in addressing urban flood risk[1].

However, recent studies have reminded us that the spatial redistribution of hydrological processes may also lead to new forms of risk inequality. Kumar et al.[52], in their latest study of Surat, India, found that while certain embankments reduced flood damage in the urban core, they intensified flood severity in downstream areas and significantly increased disparities in exposure and losses. It is therefore essential for planning processes to carefully account for such potential trade-offs.

In the scenario-based analysis of future SSPs, our simulations show that the rapid increase in both asset and population exposure significantly undermines the mitigating effects of urban planning. This simulation-based finding aligns with earlier studies, which underscore the need for intervention measures that are integrated with broader socioeconomic development pathways[53–57]. Nevertheless, by incorporating urban planning, our simulation results indicate a more optimistic outlook compared to previous studies.

The broader governance literature highlights that a more pressing challenge lies in the inability to translate high-level goals into spatially and institutionally grounded actions[58,59]. The existing planning for flood resilience remains limited to abstract goal-setting and indicator constraints, lacking concrete implementation and incentive mechanisms, technical standards, as well as platforms for cross-sectoral coordination and dialogue[60,61]. Additionally, the absence of monitoring and feedback mechanisms in implementation processes makes it difficult for planning to adjust and correct itself in response to changes. Under fiscal constraints, economic growth imperatives, and rigid performance evaluation systems, adaptation planning is frequently sidelined in day-to-day governance[62]. Functional fragmentation has also weakened the authority of planning agencies, making it difficult to generate the sustained political commitment and operational momentum required for transformative adaptation[13,62]. Against this backdrop, for urban planning to truly fulfill its regulatory and adaptive functions, it must be re-envisioned not merely as a regulatory tool for static spatial control but as a governance instrument that possesses temporal sequencing, responsiveness, and systemic nesting capacities.

Drawing on both our simulation results and insights from the broader literature, we propose policy recommendations to strengthen the regulatory capacity of urban planning for future flood risk management. First, aligning risk management with broader socioeconomic development paths is crucial to prevent planning from being sidelined amid rapid urbanization and resource shifts[28]. Second, adaptive urban measures need clearer spatial guidance, shifting from vision-based to operation-oriented planning. This requires stronger cross-departmental coordination and policy integration across ecological protection, urban renewal, and drainage to ensure spatial alignment and complementarity[63]. Third, linking urban and regional scales is vital, especially in the Pearl River Delta, where integrated catchment-scale planning can coordinate upstream and downstream adaptive actions. Finally, we recommend a dynamic feedback system using spatial data to connect risk assessment, implementation monitoring, and planning updates. Remote sensing, waterlogging records, and more sophisticated inclusion of risk-reduction measures can track adaptation progress and flood risk changes, supporting evidence-based plan revisions and bridging gaps between planning on paper and real-world outcomes[64]. This will strengthen planning as a tool for resilient governance.

Our modeling approach contributes to bridging the evaluation divide between policy intent and actual spatial outcomes, particularly through integrating multi-source data and simulating the effects of extreme climate scenarios and policy interventions. Moving forward, it is necessary to further develop such models into feedback-enabled tools that incorporate policy implementation progress and environmental changes, thereby more accurately portraying the evolution of risks and adaptation pathways in complex urban systems. In addition, our simulations do not explicitly account for socioeconomic planning measures such as urban renewal programs, slum upgrading initiatives, prioritizing vulnerable groups, or directing interventions toward high-exposure areas. Future research should aim to integrate socioeconomic dimensions more explicitly into modeling frameworks to improve the accuracy of risk evaluations.

It should be noted that some of the findings discussed in this section are directly derived from our simulation results. For instance, the importance of rapid drainage infrastructure, the hydrological buffering function of ecological spaces, the redistribution of runoff through spatial planning, and the mitigating effect of planning strategies on rising hazard and exposure were tested and visualized through scenario-based analysis. These results demonstrate how specific spatial planning interventions can influence local flood dynamics and future risks. In contrast, challenges such as the absence of feedback mechanisms and the gap between policy goals and on-the-ground implementation are primarily drawn from the literature and were not explicitly modeled in this study. While our analysis highlights the importance of addressing these governance and institutional issues, their changing relationship with planning processes and flood resilience outcomes still requires further exploration in future research.

In conclusion, by incorporating actual planning measures and conducting multi-scenario simulation assessments, this study demonstrates the technical capacity of urban planning to reduce flood risks. While urban planning can spatially mitigate hazard and exposure, its effectiveness ultimately depends on broader socioeconomic development pathways and the extent to which planned spatial strategies are implemented in practice. The study also underscores the value of policy-integrated modeling in advancing adaptation assessment and improving the linkage between planning intentions and on-the-ground outcomes.

Methods

Methodological framework

This study establishes an integrated modeling framework to assess future urban flood hazard and exposure under different climate and planning scenarios. As shown in Fig. 9, the framework combines climate scenario design, hydrological modeling, and spatial parameterization of urban planning strategies. Rainfall scenarios are constructed based on bias-corrected CMIP6 data and regional Intensity-Duration-Frequency (IDF) curves, providing input to the hydrological simulation. The CADDIES (Cellular Automata Dual-Drainage Simulation)-2D model is employed to simulate flood dynamics, incorporating surface characteristics such as land use, elevation, and buildings. Planning interventions, identified through a review of planning documents, are grouped into functional categories and translated into modified land use layers with assigned hydrological parameters. This parameterization bridges policy intent and hydrological behavior, enabling the simulation of planning effects on flood hazards. Future hazard maps are generated for multiple SSP scenarios, both with and without planning considerations.

The study area is the PRDM region in southern China, one of the most densely urbanized and economically dynamic regions worldwide. The region is situated on extensive low-lying floodplains and is subject to a subtropical monsoon climate that produces frequent episodes of short-duration extreme rainfall, rendering it highly susceptible to pluvial flooding. In recent years, the PRDM has implemented a portfolio of planning measures, including ecological restoration projects, flood-control infrastructure, and sponge city initiatives, providing an ideal context to assess how planning strategies interact with climate change and socioeconomic development pathways.

The following sections detail all components within the modeling framework.

Parameterization of urban planning strategies

The parameterization of urban planning strategies forms the basis of the model's scenario design and analysis, as it relies directly on the processing of land-cover data. For the baseline, land-cover information was obtained from the Esri Sentinel-2 Land Cover Explorer. The dataset comprises nine classes, including water, forest, cropland, and built-up areas. The

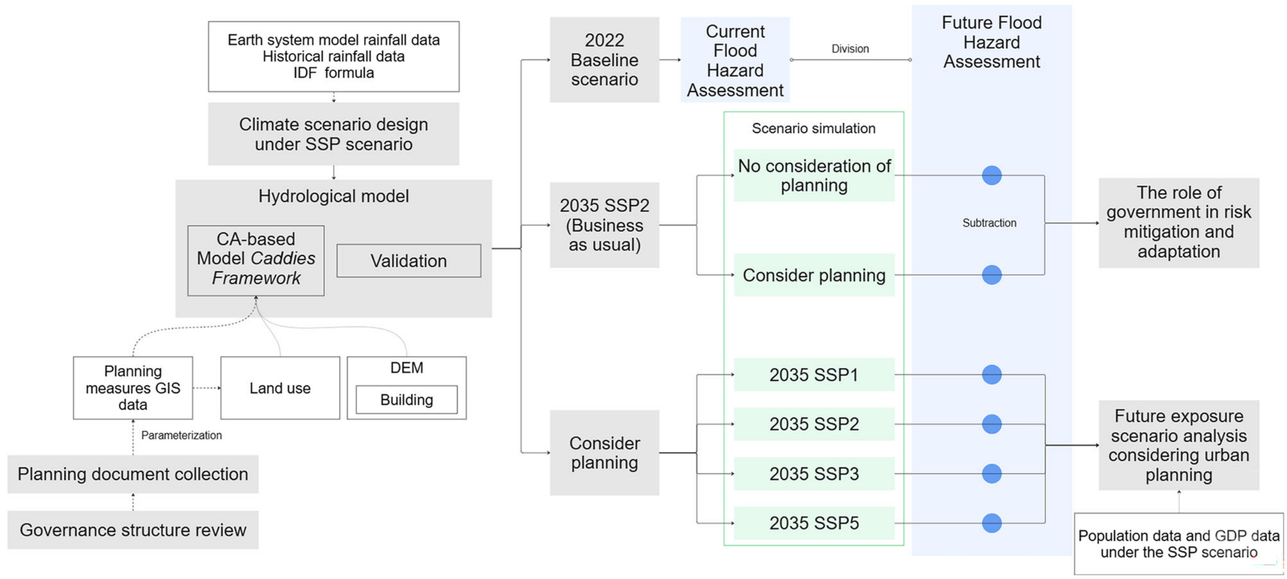

Fig. 9 | Workflow of the integrated modeling framework. This figure shows the integrated modeling framework combining climate scenario design, hydrological simulation with CADDIES-2D, and spatial parameterization of urban planning strategies to assess future flood hazard and exposure.

Table 1 | Classification of planned land use types

Code	Land use type	Description (Including Representative Planning Measures)
101	Planned Wetland	Newly planned wetland areas (e.g., wetland parks, flood retention wetlands)
102	Planned Green Corridor	Linear infiltration zones, such as urban greenways and ecological corridors
103	New Drainage Channel	Newly planned rivers or flood discharge channels for rapid runoff conveyance
104	Ecological Restoration	Ecological restoration areas (e.g., reforestation, ecological buffer zones)
105	Urban Storage Area	Areas designated for storage ponds or stormwater regulation facilities (area-based representation)
106	Sponge City Zone	Areas with enhanced infiltration capacity through sponge city measures like permeable pavements and rain gardens

hydrological parameters associated with these land use types were referenced from Xu et al.[65] (Table 1). The 2035 scenario incorporates spatial adjustments derived from planning measures.

The planning measures were identified through an extensive review of local planning documents. From these documents, we selected six planning types that met two criteria: (1) clear spatial boundaries, and (2) explicit flood mitigation functions. These planning measures encompass a range of ecological and engineered strategies designed to mitigate urban flood risks. Infiltration-enhancing interventions, such as urban green parks, greenways, ecological restoration zones, and sponge city infrastructure, increase permeable surface areas and reduce imperviousness, thereby lowering surface runoff and delaying peak flows. Measures aimed at improving drainage capacity, including newly planned floodways and runoff channels, strengthen flow pathways during extreme rainfall events, particularly in flood-prone zones. Engineering-based drainage upgrades, such as enhanced pipelines, pumping stations, and storage basins, further expand short-term drainage and retention capacity to alleviate pluvial flooding. In addition, the expansion of conveyance zones through blue corridors, minor waterways, and artificial wetlands enhances hydrological connectivity and flow continuity at key nodes within the urban system.

Based on the explicit spatial delineation of the six planning types, we incorporated them as additional land-cover categories and overlaid them onto the baseline land-cover map to produce the 2035 land-cover data.

Hydrological parameters, including infiltration rates and Manning's roughness coefficients, were determined for the six additional land use categories through a structured range-based procedure. We first compiled plausible parameter ranges from hydrological experiments, design manuals, and previous modelling studies for surface types comparable to the planned measures[12,20,66–70]. Within these ranges, we then selected specific values that reflect the relative permeability and surface roughness of each planned land cover type in comparison with the classes reported in Table 1, ensuring internal consistency across all land use categories.

For planned wetlands, green corridors, and ecological restoration zones, the chosen infiltration and roughness values correspond to documented intervals for shallow retention areas and low disturbance vegetated surfaces. In contrast, coefficients for urban storage areas, new drainage channels, and sponge city zones were determined with reference to standard design specifications for detention basins, engineered conveyance channels, and low-impact development facilities, which provide established parameter ranges for infiltration performance and hydraulic resistance. The final numerical values and their justifications are reported in Table 2.

Scenario design for rainfall inputs

The rainfall inputs used in the flood simulations were developed through a multi-stage procedure that integrates bias-corrected CMIP6 precipitation, IDF calibration, and standardized design-storm generation. Daily precipitation from the BCC-CSM2-MR model was first corrected using the Empirical Quantile Mapping (EQM) method to align modeled and observed rainfall distributions. The corrected time series were then assembled into baseline and future climate datasets and used to derive scenario-specific IDF curves through nonlinear parameter fitting and subsequent normalization to ensure comparability across scenarios. Finally, the normalized IDF relationships were converted into high-resolution rainfall time series using the Chicago Design Storm method, generating consistent extreme rainfall inputs for all flood-model simulations. The specific process is as follows.

Table 2 | Parameterization of planned land cover types

New land cover type	Infiltration rate (mm/h)	Estimation basis/justification	Roughness (*n*)	Estimation basis/justification
Planned Wetland	3.0	Between paddy fields and flooded vegetation; typically shallow water retention areas	0.080	Similar to flooded vegetation
Ecological Restoration	2.8	Mostly low-disturbance grassland or shrubland; between broomgrass and moderately disturbed forest	0.070	Lower than trees, higher than rangeland
New Drainage Channel	0.5	Engineered bare riverbed with generally low permeability; designed mainly for rapid runoff	0.030	Close to water, but slightly higher due to partially rough channel beds
Urban Storage Area	2.0	Mostly non-permeable basins, but with vegetated retention zones at edges; moderate infiltration	0.040	Smooth basin slopes with localized drainage outlets; lower than water
Sponge City Zone	2.5	Mixed permeable pavement and rain gardens; higher than built-up areas, lower than grassland	0.100	Moderate resistance of artificial permeable surfaces; lower than trees, higher than grassland
Planned Green Corridor	2.6	Mixed shrub-grass areas, similar to ecological restoration zones	0.075	Between rangeland and ecological restoration

Table 3 | Relative rainfall ratio for various durations

Duration (hours)	1	2	3	6	12	24
Rainfall Ratio (relative to P24)	0.059	0.115	0.170	0.323	0.589	1.000

First, daily precipitation data from the BCC-CSM2-MR Earth System Model were obtained for the study area from the Copernicus Climate Data Store. Model biases were corrected using the EQM method[71,72]. EQM adjusts each quantile of the modeled rainfall distribution to match the corresponding observed quantile, thereby correcting systematic biases while preserving the temporal variability of the original series. This correction was applied across the full rainfall distribution, ensuring consistency in mean, variance, and extremes. The observed reference dataset was daily rainfall from the China Meteorological Administration for 2004–2013.

Second, the EQM-corrected historical and future simulations were assembled into two series:

1. Baseline period (2003–2022): Data before 2015 were taken from the historical simulation, and data from 2015 onward were derived from the SSP2-RCP4.5 pathway. This dataset represents the present-day climate conditions.
2. Projection period (2016–2035): Data were derived from four SSP-RCP pathways: SSP1-RCP1.26, SSP2-RCP2.45, SSP3-RCP3.70, and SSP5-RCP5.85.

Third, the EQM-corrected daily rainfall series for each SSP scenario was used to calibrate the corresponding IDF curve. Specifically, the annual maximum daily precipitation was extracted to estimate the multi-year average of 24-hour design rainfall (P24). Using an empirical ratio method, rainfall depths for different durations (1, 2, 3, 6, 12, and 24 h) were scaled relative to P24 based on a standard reference curve (the 2022 design formula), as shown in Table 3. These ratios were used to construct the IDF fitting functions as shown in Eq. (1).

$$i(t,T) = \frac{a \cdot T^n}{(t+b)^c} \tag{1}$$

where $T = 100$ years represents the return period. Parameters a, b, c, and n were calibrated using nonlinear least squares fitting. This procedure links the frequency of extreme rainfall to storm duration through a unified functional form, enabling the calibrated parameters to capture both intensity scaling with return period and the temporal structure of rainfall across durations.

Fourth, to ensure comparability between future and current IDF curves, the fitted parameters were further structurally aligned and scaled using a linear normalization of the $a\ T^n$ term. The normalization ensures that differences among scenarios arise from climate-driven changes in rainfall statistics rather than arbitrary shifts in fitted parameters, thereby preserving the physical comparability of the IDF curves. The final 100-year rainfall intensity equations for each SSP-RCP scenario are summarized in Table 4.

Last, using the calibrated IDF formulas, the Chicago Design Storm method was applied to generate rainfall intensity time series at 1-min resolution for use as input in the flood simulation model. The peak intensity was positioned at 40% of the total storm duration (i.e., $r = 0.4$), and the total design duration was set to 60 min.

Flood simulation model

CADDIES-2D is a two-dimensional pluvial flood simulation model developed by the University of Exeter, UK[73–75]. This model utilizes infiltration rates and roughness of different land cover types to represent the urban drainage system. It employs Cellular Automata (CA) technology instead of solving shallow water equations, which significantly reduces computational load and improves efficiency[73]. CA models represent space as discrete grid

Table 4 | IDFs of 100-year rainfall for various scenarios

Scenario	IDF
Baseline	$i(t,100) = \frac{104.92}{(t+43.589)^{0.826}}$
2035 SSP1-RCP1.26	$i(t,100) = \frac{97.62}{(t+43.589)^{0.826}}$
2035 SSP2-RCP2.45	$i(t,100) = \frac{105.48}{(t+43.589)^{0.826}}$
2035 SSP3-RCP3.70	$i(t,100) = \frac{106.80}{(t+43.589)^{0.826}}$
2035 SSP5-RCP5.85	$i(t,100) = \frac{113.31}{(t+43.589)^{0.826}}$

Table 5 | Performance metrics for calibration of resampling methods

Method name	Pixel-level accuracy (%)	RMSE	MAE
Block_Average	80.37	0.2376	0.1268
INTER_AREA	79.08	0.2476	0.1348
INTER_LANCZOS4	76.96	0.2872	0.1533
PyrDown	78.99	0.2465	0.1342
Average_Pooling	79.63	0.2415	0.1307

cells and update their states based on simple local transition rules[76–78]. This bottom-up approach has been widely applied in urban growth and hydrological modeling because of its ability to capture complex spatial dynamics with relatively low computational demand[74].

Besides the fast computational speed, another advantage of using this model is its lower requirement for accurate drainage network data, which is often unavailable in many cities[75,79]. Despite the reduced dependency on detailed drainage network information, the model maintains a high level of accuracy, which has been validated by numerous studies across various cities worldwide, such as in the UK[80,81], China[41,70,82], and Iran[83].

The input data for CADDIES-2D model includes Digital Elevation Model (DEM), land cover data, and designed rainfall scenarios. The 30-m horizontal resolution DEM was obtained from FABDEM V1-2 data[84]. The DEM data was further overlaid with CBRA building data[85] to ensure that floodwaters could not flow through building areas in the simulation. In the model, the computational unit is set to 100 × 100 m. All input datasets were resampled accordingly to match the 100-m grid.

To evaluate the reliability of the flood model outputs, we conducted a spatial comparison between the maximum water depth simulated by our model and reference data from a representative 100-year return period rainfall scenario provided in the UrbanFlood24 dataset developed by Cao et al.[86]. The comparison was performed within the urban spatial extent specified in the dataset.

UrbanFlood24 is a high-resolution urban flood simulation dataset developed using a deep learning–based model. It operates on a 2-m spatial resolution over 500 × 500 raster grids, enabling detailed representation of surface water accumulation in complex urban environments. Due to the mismatch in spatial resolution between our flood model outputs and the UrbanFlood24 validation dataset, we employed a series of commonly used raster resampling techniques, including cv2.INTER_AREA, cv2.INTER_LANCZOS4, pyrDown, block average, and average pooling, to harmonize both outputs to a 30-m resolution. Performance was then assessed using three standard metrics: pixel-level accuracy, Root Mean Square Error (RMSE), and Mean Absolute Error (MAE).

Among all methods tested, the block average approach yielded the best validation results: Pixel-level accuracy reached 80.37%, indicating that over 80% of simulated grid cells deviated from the reference values by less than ±0.2 m; RMSE was 0.2376 m, suggesting limited deviation in high-error zones; MAE was 0.1268 m, implying an average per-pixel error of approximately 13 cm. Validation results across all five resampling methods are presented in Table 5. The slight differences among methods confirm that the model results are robust to resampling choices.

Although the spatial resolution of our model is lower than that of the U-RNN model used in UrbanFlood24, the high consistency in spatial inundation structure and depth distribution confirms the robustness of our flood model for scenario-based urban flood risk assessment.

Estimation of population distribution and exposure assessment

Following the IPCC AR6, flood risk arises from the interaction of hazard (the potentially damaging physical event), exposure (people or assets in harm's way), and vulnerability (the propensity to be adversely affected)[87]. Hazard is widely recognized as the most critical factor determining flood damage[88–90]. Exposure is often quantified as the number of people or assets intersecting the hazard extent[34,91,92]. At the same time, in some studies, it has been subsumed under vulnerability, leading to risk being expressed as the product of hazard and vulnerability[44,90,93].

As this study does not explicitly model social or structural vulnerability (e.g., vulnerability curves or socioeconomic sensitivity), we avoid labeling our indicators as "risk" in the strict sense. We only use "hazard" and "exposure" throughout the study. This is consistent with established frameworks while acknowledging that a comprehensive risk assessment would require explicit vulnerability modeling (e.g., indices or damage functions).

Specifically, we report (i) hazard, represented by simulated maximum water depth, and (ii) exposure, represented as population or asset values weighted by hazard intensity[92,94,95]. Population exposure is defined as the product of population and flood depth, while asset exposure is defined as the product of GDP and flood depth. This method extends the common practice of overlaying population or assets with hazard extent by explicitly incorporating hazard intensity, thereby producing a more refined indicator that captures not only how many people are affected but also the severity of their potential impacts[92].

To evaluate population exposure under multiple future scenarios, we constructed high-resolution population and GDP grids for the study area for the year 2035. For population, we followed the approach of Chen et al.[96]. First, we directly adopted the total regional population projected by Chen et al. for each SSP scenario. Second, the projected population was spatially redistributed across grid cells using a weighting scheme based on grid-level urbanization potential, under the assumption that cells with higher urbanization potential will attract a larger share of future population. Third, the resulting weights were normalized to produce a complete 100-m population surface for each scenario. For GDP, we applied a resampling procedure to the gridded projections provided by Wang and Sun[97].

Chen et al.[96] provide a valuable 1-km resolution population dataset for China, which incorporates essential demographic parameters such as age structure, fertility, mortality, and migration patterns. Following Chen et al., the SSP scenarios govern demographic processes such as age structure, fertility, mortality, and migration, and therefore determine the total population size rather than its spatial distribution. In contrast, spatial patterns of population are shaped by the RCP-linked urban development pathways. This distinction implies that SSP-projected population totals can be consistently combined with alternative urbanization fractions to generate population distributions aligned with the specific RCP scenarios. This approach assumes that grid-level urbanization potential is the primary driver of future population concentration.

Since the RCP pathways used in their allocation differ from those employed in our rainfall scenario design based on the Earth system model, directly using them would cause inconsistencies. Accordingly, we used the regional population totals from Chen et al. together with the urbanization data of He et al.[98] to generate population distributions consistent with the SSP–RCP scenarios required in this study. This also enables us to assess population exposure at a finer 100-m resolution, aligning it with the outputs of the flood model. To remain consistent with the SSP projections, we keep the regional population totals fixed for each scenario and adjust only their spatial distribution.

Specifically, we first used the 2020 population data from WorldPop at a resolution of 100 m as the spatial reference layer. In parallel, urbanization ratios for 2035 under four SSP-RCP scenarios were obtained from the dataset provided by He et al.[98]. These ratios represent the urbanization potential of each grid cell on a scale from zero to one hundred percent. To ensure spatial alignment between datasets, the urbanization data were resampled to match the WorldPop grid resolution. When differences in spatial referencing occurred, affine transformation and coordinate reprojection were applied.

A spatially weighted redistribution model was then constructed to allocate the projected total provincial population to each raster cell. The model accounted for both the original population density and the urbanization potential of each cell using the weighting function shown in Eq. (2).

$$W_i = P_i \cdot U_i \tag{2}$$

where W_i denotes the allocation weight for cell, P_i is the initial population density from the WorldPop dataset, and U_i is the normalized urbanization potential ranging from zero to one. After normalization, the population value for each cell was calculated as shown in Eq. (3).

$$\hat{P}_i = \frac{W_i}{\sum_j^0 W_j} \cdot P_{\text{total}} \tag{3}$$

where P_{total} represents the total population projected for the corresponding SSP scenario. Using this approach, we first generated a complete population surface for the entire Guangdong province and subsequently extracted the portion corresponding to the PRDM region. For the baseline scenario, we used population projections for the year 2022 under SSP2.

To quantify population exposure, we overlaid the high-resolution population grids for each scenario with the corresponding maximum flood depth outputs from the simulation model. Population exposure was calculated as the product of the water depth and the number of people affected in each grid cell.

The GDP data used in this study is derived from the gridded global GDP dataset under SSP scenarios developed by Wang and Sun[97], covering projections for the year 2035 under SSP1, SSP2, SSP3, and SSP5. The original spatial resolution is 1 km, and it was resampled using the nearest neighbor method to match the 100 m resolution. To avoid artificial inflation of total values during resampling, each original 1 km grid cell value was evenly distributed across the corresponding 100 grid cells at 100 m resolution. In this process, we retain the scenario-specific total GDP and adjust only its spatial allocation. Asset exposure was calculated as the product of water depth and GDP value in each grid cell.

For comparative analysis between future scenarios and the baseline, we applied a ratio-based method: hazard, population exposure, and asset exposure values under each future scenario were divided by the corresponding values under the 2022 baseline scenario at the grid level. The resulting ratios (hazard ratio, population exposure ratio, and asset exposure ratio) indicate relative change: values greater than 1 denote an increase, values less than 1 indicate a decrease, and values equal to 1 reflect no change.

Methodological limitations

Despite efforts made to ensure the systematic and practical nature of the methods in model construction, data integration, and spatial processing, this study has several limitations. First, the parameterization of urban planning relied primarily on plan types with clearly defined boundaries and spatial representations, which limited the inclusion of policy measures that lacked geographic expression or existed only as abstract concepts. In addition, to standardize land use processing, some planning measures with composite functions or locally varying attributes were simplified into single land use categories, which may not fully reflect their actual hydrological response mechanisms or spatiotemporal heterogeneity of effects.

Second, although the overall hydrodynamic structure and spatial patterns of the model were validated using high-resolution datasets, the simulation's resolution of 100 meters remains insufficient to capture the influence of micro-topography or drainage infrastructure layout, particularly in older urban districts and newly developed high-density zones. The flood model does not explicitly represent detailed underground drainage networks, which may affect the accuracy of flow routing and localized inundation.

Lastly, in exposure assessment, the spatial redistribution of population and GDP mainly relied on prior distributions and adjustments based on urbanization potential. While this approach ensured consistency in total quantity and spatial alignment, it did not capture dynamic processes such as migration or functional transformation. Therefore, the resulting exposure estimates are more suitable for structural comparisons than for fine-scale quantification.

In summary, although this study developed an integrated spatial simulation framework that combines climate, planning, and exposure data, the results should be understood as identifying policy effects and trend patterns under assumed constraints, rather than providing precise predictions of future flood impacts.

Data availability

All datasets used in this study are publicly available from the sources listed below. Land cover data is obtained from the Esri Sentinel-2 Land Cover Explorer (https://livingatlas.arcgis.com/landcover/). Daily precipitation data is obtained from the Copernicus Climate Data Store (https://cds.climate.copernicus.eu/datasets). Observational daily precipitation data is from the China Meteorological Data Service Centre (https://data.cma.cn/). DEM data is obtained from the FABDEM V1.2 dataset (https://data.bris.ac.uk/data/dataset/s5hqmjcdj8yo2ibzi9b4ew3sn) and overlaid with CBRA building data (https://zenodo.org/records/7500612). Model validation reference data is from a representative 100-year return period rainfall scenario provided in the UrbanFlood24 dataset (https://holmescao.github.io/datasets/urbanflood24). Population distribution data is obtained from WorldPop (https://hub.worldpop.org/project/categories?id=3). Future population projections under SSP scenarios are sourced from Chen et al. (2020) (https://doi.org/10.6084/m9.figshare.11898405). Urban fractional change data for downscaling future population under SSP scenarios is obtained from Yu et al. (2023) (https://doi.org/10.6084/m9.figshare.20391117.v4). Gridded global GDP projections under SSP scenarios are obtained Wang and Sun (https://zenodo.org/records/7898409). All processed data and simulation outputs generated during this study are available from the corresponding authors upon reasonable request.

Code availability

The code that supports the findings of this study is available upon request from the corresponding authors.

Received: 23 June 2025; Accepted: 1 February 2026;
Published online: 17 February 2026

References

1. Chan, F. K. S. et al. Building resilience in Asian mega-deltas. *Nat. Rev. Earth Environ.* **5**, 522–537 (2024).
2. Chan, F. K. S. et al. Comparison of sustainable flood risk management by four countries – the United Kingdom, the Netherlands, the United States, and Japan – and the implications for Asian coastal megacities. *Nat. Hazards Earth Syst. Sci.* **22**, 2567–2588 (2022).
3. Berrang-Ford, L. et al. A systematic global stocktake of evidence on human adaptation to climate change. *Nat. Clim. Chang.* **11**, 989–1000 (2021).
4. Yang, L. E., Chen, J., Geng, J., Fang, Y. & Yang, W. Social resilience and its scale effects along the historical Tea-Horse Road. *Environ. Res. Lett.* **16**, 045001 (2021).

5. Berrang-Ford, L. et al. Tracking global climate change adaptation among governments. *Nat. Clim. Chang.* **9**, 440–449 (2019).
6. Wannewitz, M. et al. Progress and gaps in climate change adaptation in coastal cities across the globe. *Nature cities.* **1**, 610–619 (2024).
7. Petzold, J. et al. A global assessment of actors and their roles in climate change adaptation. *Nat. Clim. Chang.* **13**, 1250–1257 (2023).
8. van Stigt, R., Driessen, P. P. J. & Spit, T. J. M. A user perspective on the gap between science and decision-making. Local administrators' views on expert knowledge in urban planning. *Environ. Sci. Policy* **47**, 167–176 (2015).
9. Kauark-Fontes, B., Marchetti, L. & Salbitano, F. Integration of nature-based solutions (NBS) in local policy and planning toward transformative change. Evidence from Barcelona, Lisbon, and Turin. *Ecol. Soc.* **28**, 8 (2023).
10. Otto, A., Haupt, W., Eckersley, P., Kern, K. & Thieken, A. H. Dynamism and stasis in the climate policies of German cities between 2018 and 2022. *Mitig. Adapt Strateg Glob. Change* **30**, 30 (2025).
11. Reckien, D. et al. Quality of urban climate adaptation plans over time. *npj Urban Sustain* **3**, 13 (2023).
12. Feng, W. et al. Synergizing Flood Mitigation and Water Quality Goals through Green Infrastructure in Dali City, China. *Int. J. Disaster Risk Reduction* 105785 https://doi.org/10.1016/j.ijdrr.2025.105785 (2025).
13. Liss, B. M. et al. Mainstreaming climate change adaptation into urban planning—A pragmatic protocol to tackle the implementation gap. *Front. Clim*. **7**, 1557352 (2025).
14. Reckien, D. et al. How are cities planning to respond to climate change? Assessment of local climate plans from 885 cities in the EU-28. *J. Clean. Prod.* **191**, 207–219 (2018).
15. Salvia, M. et al. Will climate mitigation ambitions lead to carbon neutrality? An analysis of the local-level plans of 327 cities in the EU. *Renew. Sustain. Energy Rev.* **135**, 110253 (2021).
16. Eisenack, K. & Roggero, M. Many roads to Paris: explaining urban climate action in 885 European cities. *Glob. Environ. Change* **72**, 102439 (2022).
17. Du, S. et al. Hard or soft flood adaptation? Advantages of a hybrid strategy for Shanghai. *Glob. Environ. Change* **61**, 102037 (2020).
18. Yin, D. et al. Can flood resilience of green-grey-blue system cope with future uncertainty? *Water Res.* **242**, 120315 (2023).
19. Yang, Y., Yin, J., Feng, W., Yang, L. E. & Wang, J. Dynamic flood evacuation modelling for coastal cities: a case study of Shanghai. *Int. J. Disaster Risk Reduct.* **125**, 105591 (2025).
20. Qin, H., Li, Z. & Fu, G. The effects of low impact development on urban flooding under different rainfall characteristics. *J. Environ. Manag.* **129**, 577–585 (2013).
21. Wang, Y., Peng, L., Yang, L. E., Wang, Z. & Deng, X. Attributing effects of classified infrastructure management on mitigating urban flood risks: a case study in Beijing, China. *Sustain. Cities Soc.* **101**, 105141 (2024).
22. Yang, L. E., Weinelt, M., Unkel, I. & Petrie, C. A. Social resilience to changes in climate over the past 5000 years. *Environ. Res. Lett.* **19**, 120201 (2024).
23. Peng, L., Wang, Y., Yang, L., Garchagen, M. & Deng, X. A comparative analysis on flood risk assessment and management performances between Beijing and Munich. *Environ. Impact Assess. Rev.* **104**, 107319 (2024).
24. Ho, T. P. et al. A systematic investigation of flood resilience measures in the Mekong River Basin. *Environ. Sci. Policy.* **172**, 104228. (2025).
25. Ho, T. P. et al. A Bayesian network analysis on the interactions of flood resilience measures in the Vietnamese Mekong Delta. *Environ. Res. Lett.* **21**, (2026).
26. Meng, M., Dabrowski, M. & Stead, D. Enhancing flood resilience and climate adaptation: the state of the art and new directions for spatial planning. *Sustainability* **12**, 7864 (2020).
27. Zhai, G., Li, S. & Chen, J. Reducing urban disaster risk by improving resilience in china from a planning perspective. *Hum. Ecol. Risk Assess. Int. J.* **21**, 1206–1217 (2015).
28. Wu, Y. et al. Sustainable urban planning to control flood exposure in the coastal zones of China. *Landsc. Ecol.* **39**, 141 (2024).
29. Wang, Y., Liu, C., Wang, Y., Liu, Y. & Liu, T. Climate risk assessment and adaption ability in China's coastal urban agglomerations - A case study of Guangdong-Hong Kong-Macao greater bay area. *J. Clean. Prod.* **452**, 142036 (2024).
30. Zhou, S. et al. Quantifying the spatiotemporal dynamics of urban flooding susceptibility in the greater bay area under shared socio-economic pathways using the SD-PLUS-LightGBM framework. *Resour., Conserv. Recycl.* **223**, 108534 (2025).
31. Oneto, G. & Canepa, M. Addressing sustainable urban flood risk: reviewing the role and scope of theoretical models and policies. *Water Policy* **25**, 797–814 (2023).
32. Harrison, P. A., Dunford, R. W., Holman, I. P. & Rounsevell, M. D. A. Climate change impact modelling needs to include cross-sectoral interactions. *Nat. Clim. Change* **6**, 885–890 (2016).
33. Birkmann, J., Welle, T., Solecki, W., Lwasa, S. & Garschagen, M. Boost resilience of small and mid-sized cities. *Nature* **537**, 605–608 (2016).
34. Rogers, J. S., Maneta, M. P., Sain, S. R., Madaus, L. E. & Hacker, J. P. The role of climate and population change in global flood exposure and vulnerability. *Nat. Commun.* **16**, 1287 (2025).
35. Dartmouth Flood Observatory. https://floodobservatory.colorado.edu/Archives/index.html.
36. Petzold, J. et al. Identifying future challenges for climate change adaptation through insights from participatory scenario-downscaling in Mumbai. *npj Clim. Action* **3**, 111 (2024).
37. Riahi, K. et al. The Shared Socioeconomic Pathways and their energy, land use, and greenhouse gas emissions implications: an overview. *Glob. Environ. Change* **42**, 153–168 (2017).
38. Vu, B. T. et al. Enablers and barriers to implementing effective disaster risk management according to good governance principles: lessons from Central Vietnam. *Int. J. Disaster Risk Reduct.* **120**, 105344 (2025).
39. Zwirglmaier, V. & Garschagen, M. Linking urban structure types and Bayesian network modelling for an integrated flood risk assessment in data-scarce mega-cities. *Urban Clim.* **56**, 102034 (2024).
40. Guerreiro, S. B., Dawson, R. J., Kilsby, C., Lewis, E. & Ford, A. Future heat-waves, droughts and floods in 571 European cities. *Environ. Res. Lett.* **13**, 034009 (2018).
41. Wang, Y., Liu, Z., Wang, G. & Xue, W. Cellular automata based framework for evaluating mitigation strategies of sponge city. *Sci. Total Environ.* **796**, 148991 (2021).
42. Sarica, G. M., Zhu, T., Jian, W., Lo, E. Y.-M. & Pan, T.-C. Spatio-temporal dynamics of flood exposure in Shenzhen from present to future. *Environ. Plan. B Urban Anal. City Sci.* **48**, 1011–1024 (2021).
43. Global temperature is likely to exceed 1.5°C above pre-industrial level temporarily in next 5 years. *World Meteorological Organization* https://wmo.int/news/media-centre/global-temperature-likely-exceed-15degc-above-pre-industrial-level-temporarily-next-5-years (2024).
44. Rey, W. et al. Assessing the impact of coastal flooding along the northern Yucatan Peninsula associated to sea level rise under different shared socio-economic pathways. *Nat. Hazards* **121**, 15443–15466 (2025).
45. Zhu, Z., Zhang, S., Zhang, Y., Yao, R. & Jin, H. Integrating flood risk assessment and management based on HV-SS model: a case study of the Pearl River Delta, China. *Int. J. Disaster Risk Reduct.* **96**, 103963 (2023).
46. Li, J., Zou, Y., Li, J. & Si, S. Urban spatial, engineering and management resilience capacity enhancement from a flood safety perspective. *Water-Energy Nexus* **7**, 213–226 (2024).
47. Wang, L. et al. A review of the flood management: from flood control to flood resilience. *Heliyon* **8**, e11763 (2022).

48. Liu, N. & Zhang, F. Urban green spaces and flood disaster management: toward sustainable urban design. *Front. Public Health* **13**, 1583978 (2025).
49. Gu, X. & Liu, X. Planning scale flood risk assessment and prediction in ultra-high density urban environments: the case of Hong Kong. *Ecol. Indic.* **162**, 112000 (2024).
50. Liao, K.-H. A theory on urban resilience to floods—a basis for alternative planning practices. *Ecol. Soc.* **17**, 4 (2012).
51. Chen, W. et al. Understanding the evolution trend of urban flood risk and resilience for better flood management. *Ecol. Indic.* **169**, 112829 (2024).
52. Kumar, A. S., Majumder, R., Kapadia, V. P. & Bhatia, U. Partial flood defenses shift risks and amplify inequality in a core–periphery city. *Nat Cities* 1–12 https://doi.org/10.1038/s44284-025-00299-7 (2025).
53. Zuo, D., Wu, C., Zheng, Y., Chen, X. & Wang, L. Climate change and human activity impacts on future flood risk in the Pearl River Delta based on the MaxEnt model. *Front. Earth Sci*. **10**, 1053829 (2023).
54. Chen, X., Zhang, H., Chen, W. & Huang, G. Urbanization and climate change impacts on future flood risk in the Pearl River Delta under shared socioeconomic pathways. *Sci. Total Environ.* **762**, 143144 (2021).
55. Yang, L., Scheffran, J., Qin, H. & You, Q. Climate-related flood risks and urban responses in the Pearl River Delta, China. *Reg. Environ. Change* **15**, 379–391 (2015).
56. Wang, M. et al. Assessing urban flooding risk in response to climate change and urbanization based on shared socio-economic pathways. *Sci. Total Environ.* **880**, 163470 (2023).
57. Hosseinzadehtalaei, P., Hamdi, R., Moradkhani, H., Termonia, P. & Tabari, H. Inequality in human exposure to future climate extremes. *Nat. Commun.* **16**, 8058 (2025).
58. Birkmann, J., Garschagen, M. & Setiadi, N. New challenges for adaptive urban governance in highly dynamic environments: revisiting planning systems and tools for adaptive and strategic planning. *Urban Clim.* **7**, 115–133 (2014).
59. Garschagen, M. Decentralizing urban disaster risk management in a centralized system? Agendas, actors and contentions in Vietnam. *Habitat Int.* **52**, 43–49 (2016).
60. Dąbrowski, M., Stead, D., He, J. & Yu, F. Adaptive capacity of the Pearl River Delta cities in the face of the growing flood risk: Institutions, ideas and interests. *Urban Stud.* **58**, 2683–2702 (2021).
61. Roy, M. et al. Quality of cities' networks of plans and prospects for flood resilience. *J. Plan. Educ. Res.* https://doi.org/10.1177/0739456X241236486 (2024).
62. Meng, M., Dąbrowski, M., Xiong, L. & Stead, D. Spatial planning in the face of flood risk: between inertia and transition. *Cities* **126**, 103702 (2022).
63. Nadin, V. Integrated, adaptive and participatory spatial planning: trends across Europe. *Regional Stud.* **55**, 791–803 (2021).
64. Newman, J. P. et al. Review of literature on decision support systems for natural hazard risk reduction: current status and future research directions. *Environ. Model. Softw.* **96**, 378–409 (2017).
65. Xu, Q., Shi, Y., Bamber, J. L., Ouyang, C. & Zhu, X. X. Large-scale flood modeling and forecasting with FloodCast. *Water Res.* **264**, 122162 (2024).
66. Fu, X. et al. Quantifying and assessing the infiltration potential of green infrastructure in urban areas using a layered hydrological model. *J. Hydrol.* **618**, 128626 (2023).
67. Eckart, K., McPhee, Z. & Bolisetti, T. Performance and implementation of low impact development – A review. *Sci. Total Environ.* **607–608**, 413–432 (2017).
68. Jia, H. et al. LID-BMPs planning for urban runoff control and the case study in China. *J. Environ. Manag.* **149**, 65–76 (2015).
69. Leng, L. et al. Performance assessment of coupled green-grey-blue systems for Sponge City construction. *Sci. Total Environ.* **728**, 138608 (2020).
70. Liu, Y. et al. Flood impact on urban transport networks considering the flooding propagation. *J. Environ. Manag.* **395**, 127972 (2025).
71. Gudmundsson, L., Bremnes, J. B., Haugen, J. E. & Engen-Skaugen, T. Technical note: downscaling RCM precipitation to the station scale using statistical transformations & a comparison of methods. *Hydrol. Earth Syst. Sci.* **16**, 3383–3390 (2012).
72. Liu, W., Zhang, X., Feng, Q. & Engel, B. A. City-scale integrated flood risk prediction under future climate change and urbanization based on the shared socioeconomic pathways (SSP) scenarios. *J. Hydrol.* **655**, 132971 (2025).
73. Guidolin, M. et al. A weighted cellular automata 2D inundation model for rapid flood analysis. *Environ. Model. Softw.* **84**, 378–394 (2016).
74. Ghimire, B. et al. Formulation of a fast 2D urban pluvial flood model using a cellular automata approach. *J. Hydroinform.* **15**, 676–686 (2012).
75. Guidolin, M. et al. CADDIES: a new framework for rapid development of parallel cellular automata algorithms for flood simulation. https://ore.exeter.ac.uk/articles/conference_contribution/CADDIES_A_New_Framework_for_Rapid_Development_of_Parallel_Cellular_Automata_Algorithms_for_Flood_Simulation/29687837/1 (2012).
76. Reimuth, A. et al. Urban growth modeling for the assessment of future climate and disaster risks: approaches, gaps and needs. *Environ. Res. Lett.* **19**, 013002 (2023).
77. Teng, J. et al. Flood inundation modelling: a review of methods, recent advances and uncertainty analysis. *Environ. Model. Softw.* **90**, 201–216 (2017).
78. Dottori, F. & Todini, E. Developments of a flood inundation model based on the cellular automata approach: Testing different methods to improve model performance. *Phys. Chem. Eart Parts A/B/C.* **36**, 266–280 (2011).
79. Gibson, M. J. et al. Accuracy and computational efficiency of 2D urban surface flood modelling based on cellular automata. *Procedia Eng.* **154**, 801–810 (2016).
80. Wang, Y. et al. An integrated framework for high-resolution urban flood modelling considering multiple information sources and urban features. *Environ. Model. Softw.* **107**, 85–95 (2018).
81. Webber, J. L. et al. Rapid assessment of surface-water flood-management options in urban catchments. *Urban Water J.* **15**, 210–217 (2018).
82. Liu, Y. et al. Flood simulation and verification in beijing urban area based on CADDIES-2D model. *Water Res. Power* **11**, 107–110. (2021).
83. Faridani, F. et al. Estimating flood characteristics using geomorphologic flood index with regards to rainfall intensity-duration-frequency-area curves and CADDIES-2D model in three Iranian basins. *Sustainability* **12**, 7371 (2020).
84. Hawker, L. et al. A 30 m global map of elevation with forests and buildings removed. *Environ. Res. Lett.* **17**, 024016 (2022).
85. Liu, Z., Tang, H., Feng, L. & Lyu, S. China Building Rooftop Area: the first multi-annual (2016–2021) and high-resolution (2.5 m) building rooftop area dataset in China derived with super-resolution segmentation from Sentinel-2 imagery. *Earth Syst. Sci. Data* **15**, 3547–3572 (2023).
86. Cao, X. et al. U-RNN high-resolution spatiotemporal nowcasting of urban flooding. *J. Hydrol.* **659**, 133117 (2025).
87. Intergovernmental Panel On Climate Change (Ipcc). *Climate Change 2022 – Impacts, Adaptation and Vulnerability: Working Group II Contribution to the Sixth Assessment Report of the Intergovernmental Panel on Climate Change* https://doi.org/10.1017/9781009325844 (Cambridge University Press, 2023).
88. Dinh, Q., Balica, S., Popescu, I. & Jonoski, A. Climate change impact on flood hazard, vulnerability and risk of the Long Xuyen Quadrangle in the Mekong Delta. *Int. J. River Basin Manag.* **10**, 103–120 (2012).

89. Balica, S. F., Popescu, I., Beevers, L. & Wright, N. G. Parametric and physically based modelling techniques for flood risk and vulnerability assessment: a comparison. *Environ. Model. Softw.* **41**, 84–92 (2013).
90. Rey, W. et al. Assessing different flood risk and damage approaches: a case of study in Progreso, Yucatan, Mexico. *J. Mar. Sci. Eng.* **8**, 137 (2020).
91. Tate, E., Rahman, M. A., Emrich, C. T. & Sampson, C. C. Flood exposure and social vulnerability in the United States. *Nat. Hazards* **106**, 435–457 (2021).
92. Lincke, D., Hinkel, J., Mengel, M. & Nicholls, R. J. Understanding the drivers of coastal flood exposure and risk from 1860 to 2100. *Earth's. Future* **10**, e2021EF002584 (2022).
93. Merz, B., Hall, J., Disse, M. & Schumann, A. Fluvial flood risk management in a changing world. *Nat. Hazards Earth Syst. Sci.* **10**, 509–527 (2010).
94. Jongman, B., Ward, P. J. & Aerts, J. C. J. H. Global exposure to river and coastal flooding: long term trends and changes. *Glob. Environ. Change* **22**, 823–835 (2012).
95. Sanders, B. F. et al. Quantifying social inequalities in flood risk. *ASCE OPEN Multidiscip. J. Civ. Eng.* **2**, 04024004 (2024).
96. Chen, Y. et al. Provincial and gridded population projection for China under shared socioeconomic pathways from 2010 to 2100. *Sci. Data* **7**, 83 (2020).
97. Wang, T. & Sun, F. Global gridded GDP data set consistent with the shared socioeconomic pathways. *Sci. Data* **9**, 221 (2022).
98. He, W. et al. Global urban fractional changes at a 1 km resolution throughout 2100 under eight scenarios of Shared Socioeconomic Pathways (SSPs) and Representative Concentration Pathways (RCPs). *Earth Syst. Sci. Data* **15**, 3623–3639 (2023).

Acknowledgements
This research has received funding from the ERC Starting Grant STORIES (Spatial-Temporal Dynamics of Flood Resilience, Grant No. 101040939), the Startup Research Funding for Introduced Talents of Nanjing University of Information Science and Technology (Grant No. 1083142501005), the Research Hub for Decarbonised Adaptable and Resilient Transport Infrastructures (DARe), funded by the UK EPSRC and the UK Department for Transport (EP/Y024257/1), the Shenzhen Science and Technology Planning Project (Grant No. KCXFZ20230731100904010), and the Innovation Team Project for General Universities in Guangdong Province, China (Grant No. 2023KCXTD050). Wenhan Feng and Anqi Zhu received funding from the LMU-CSC Scholarship.

Author contributions
W.F.: Conceptualization, methodology, software, writing—original, project coordination, visualization and spatial analysis support, formal analysis, validation. Y.L.: Software, methodology and validation, writing—original. A.Z.: Conceptualization, writing—original, data curation, resources. J.M.: Methodology and validation. T.S.: Data curation. Q.X.: Data curation. Y. Y.: Data curation. H.S.: Data curation. W.W.: Data curation. Q.Y.: Data curation. A.F.: Supervision, resources. M.G.: Supervision, resources. L.E.Y.: Conceptualization, writing—original, project coordination, supervision, resources. All authors reviewed the paper. All authors read and approved the manuscript.

Funding
Open Access funding enabled and organized by Projekt DEAL.

Competing interests
The authors declare no competing interests.

Additional information
Correspondence and requests for materials should be addressed to Wenhan Feng or Liang Emlyn Yang.